SUPPLEMENTARY INFORMATION
https://doi.org/10.1038/s41556-019-0300-y

nature cell biology

In the format provided by the authors and unedited.

A lipid-based partitioning mechanism for selective incorporation of proteins into membranes of HIV particles

Prabuddha Sengupta[1]*, Arnold Y. Seo[1], H. Amalia Pasolli[1], Yul Eum Song[2], Marc C. Johnson[2] and Jennifer Lippincott-Schwartz[1]*

[1]Howard Hughes Medical Institute, Janelia Research Campus, Ashburn, VA, USA. [2]Department of Molecular Microbiology and Immunology, Christopher S. Bond Life Sciences Center, University of Missouri, Columbia, MO, USA. *e-mail: senguptap@janelia.hhmi.org; lippincottschwartzj@janelia.hhmi.org

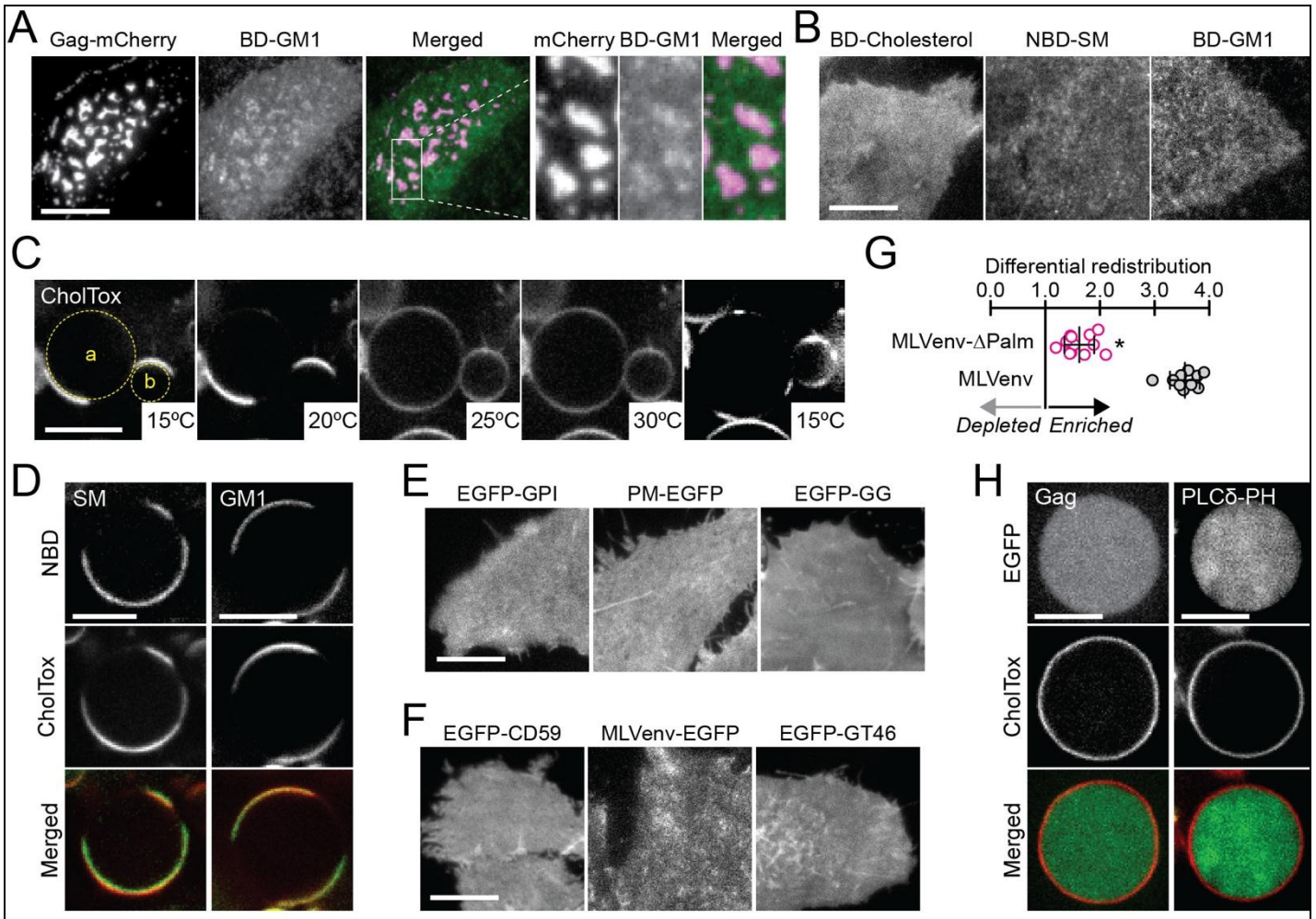

Supplementary Figure 1

Distribution of lipids and membrane proteins on HeLa cell PM and phase separated GPMVs.

(A) TIRF-M images of bodipy- GM1 (BD-GM1) distribution on PM of cells producing VLPs. VLP assembly sites are labeled by Gag-mCh. Panels at right are magnified images of boxed areas at left. (B) TIRF-M images of PM of cells labeled with BD-Ch (left), NBD-SM (middle), or BD-GM1 (right) (C) Temperature dependent reversible phase separation of GPMVs labeled with Ax555-CholTox. The dashed yellow lines on the first panel mark the perimeter of two separate phase-separated GPMVs (marked as a and b). (D) Distribution of NBD-SM and BD-GM1 in phase separated GPMVs. Ax555-CholTox labels the ordered phase of GPMVs. (E) TIRF-M images of distribution of EGFP fusions of indicated lipid-anchored proteins on PM of cells. **(**F) TIRF-M images

showing the distribution EGFP-tagged versions of indicated proteins on PM of cells. (G) Degree of enrichment of EGFP tagged MLVenv and MLVenv-ΔPalm at VLP assembly sites compared to bulk PM. Multiple cells were analyzed and data are shown as mean ± SD for *n* individual cells; two-sided Student's *t*-test, $p=3.8X10^{-13}$. *n*=10, MLVenv; *n*=12, MLVenv-ΔPalm. (H) Distribution of Gag-EGFP and PLCδ-PH-EGFP in Alexa-CholTox labeled GPMVs. (A-F, H) Representative images from two biologically independent experiments. Scale bar, 10 μm.

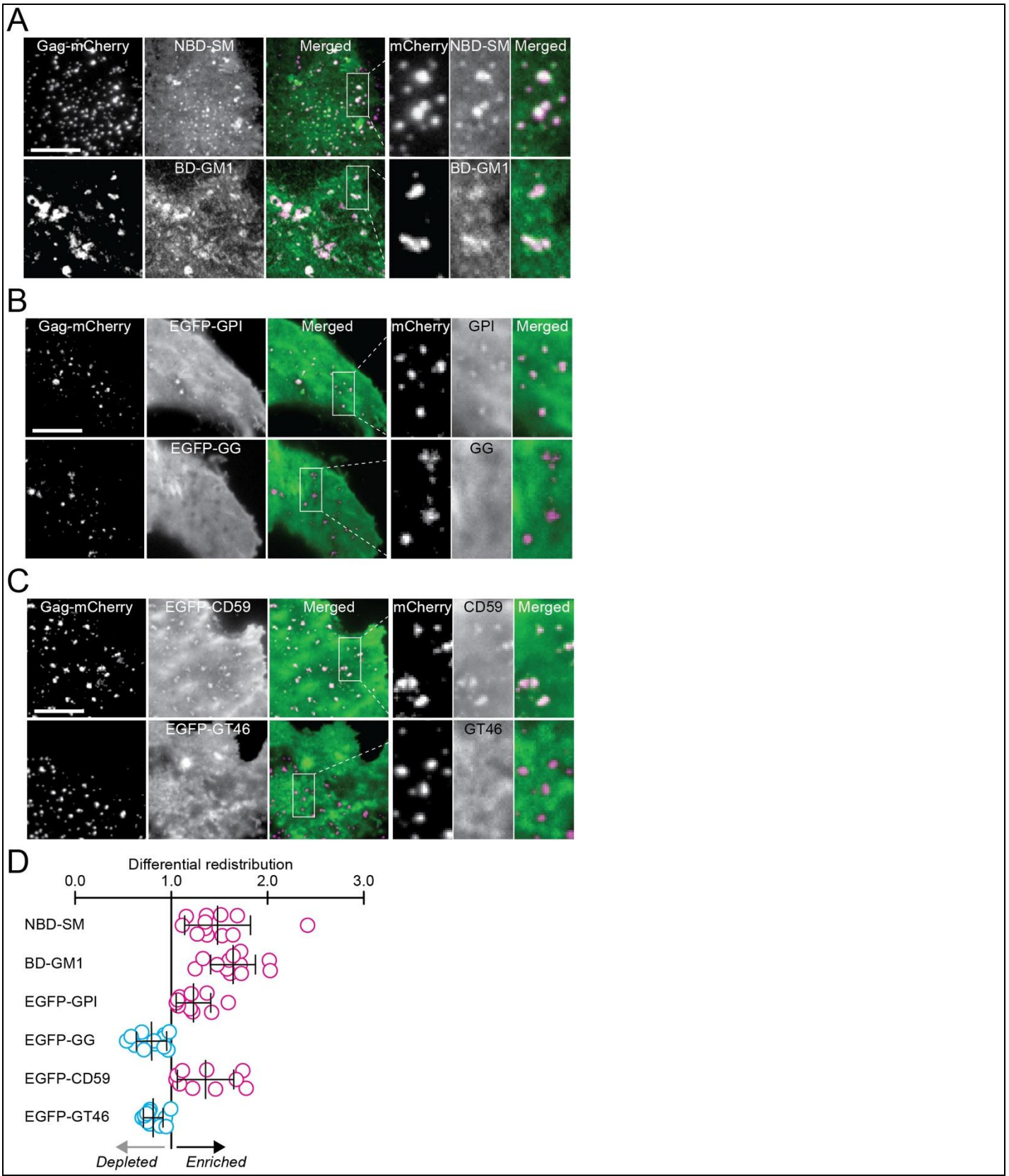

Supplementary Figure 2

Enrichment or depletion of lipids and lipid-anchored proteins at VLP assembly sites on PM of COS-7 cells correlate with their partitioning between lipid phases.

(A) TIRF-M images of NBD-SM (top) and BD-GM1 distribution on PM of COS-7 cells producing VLPs. VLP assembly sites are labeled by Gag-mCh. Panels at right are magnified images of boxed areas at left. (B) TIRF-M images of distribution of indicated lipid anchored proteins on PM of VLP producing COS-7 cells. Gag-mCh highlights VLP assembly sites. Panels at right are magnified images of boxed areas. (C) TIRF-M images showing the distribution of EGFP-fusions of indicated PM proteins during assembly of VLPs in COS-7 cells. Gag-mCh labels VLP assembly sites. Panels at right are magnified images of boxed areas. (D) Extent of enrichment or depletion of indicated lipids or proteins at VLP assembly sites compared to bulk PM. Multiple cells were analyzed for each protein and data are shown as mean ± SD for *n* individual cells. *n*=12, NBD-SM; *n*=12, BD-GM1; *n*=10, EGFP-GPI; *n*=12, EGFP-GG; *n*=10, EGFP-CD59; *n*=12, GT46. (A-C) Representative images from two biologically independent experiments. Scale bar, 10 μm.

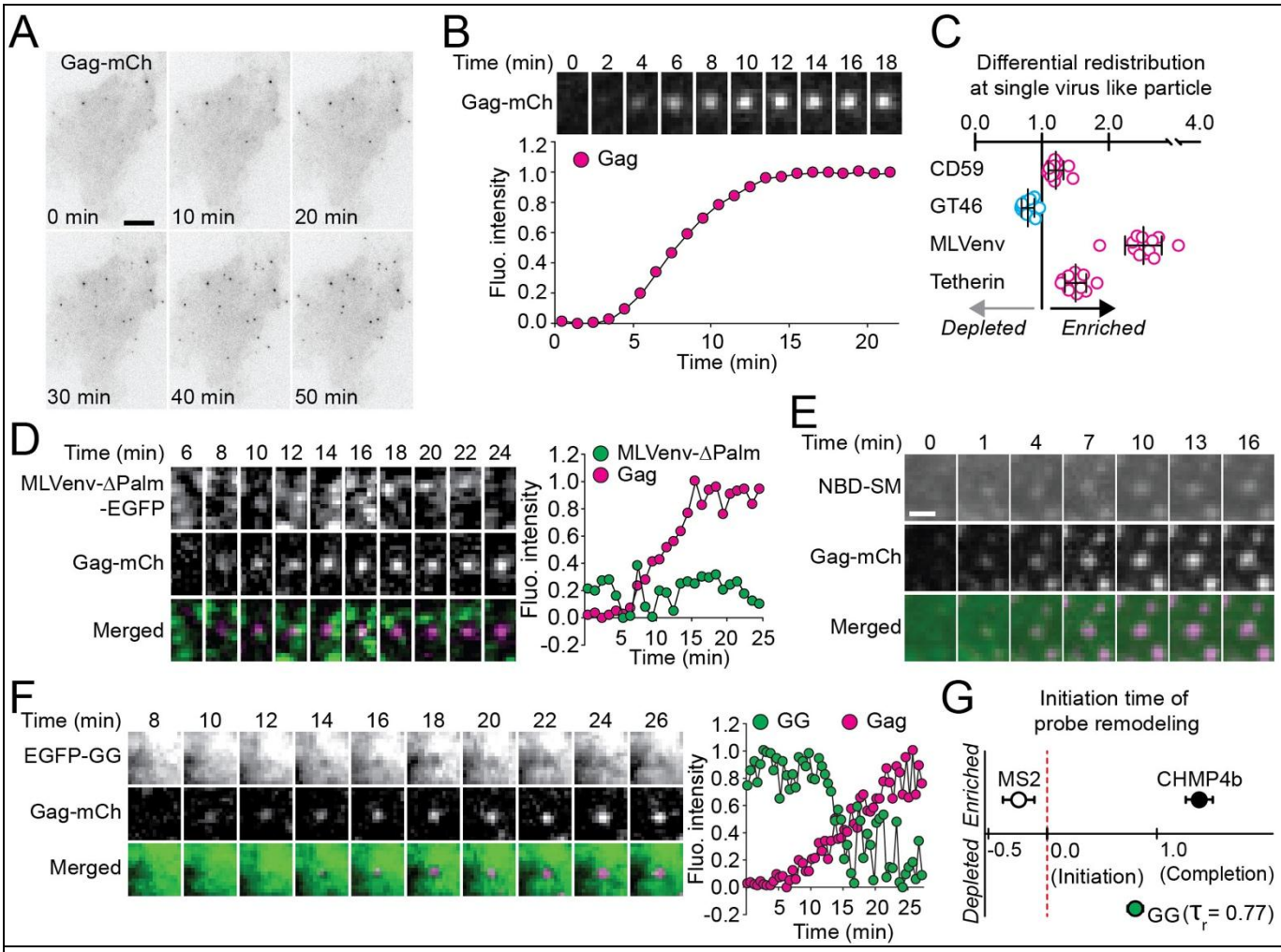

Supplementary Figure 3

Redistribution of PM proteins and lipids between bulk PM and single VLP assembly sites.

(A) Cells transfected with Gag and Gag-mCh were imaged by TIRF-M 8h post transfection. Images of a cell visualized over a 1h period showing the appearance of diffraction-limited Gag-mCh fluorescence spots marking sites of single VLP assembly. (B) (Top) Time series showing biogenesis of single VLP on PM visualized by Gag-mCh fluorescence. (Bottom) Time trace of normalized fluorescence intensity of Gag-mCh at the assembly site (shown above) during single VLP assembly. (A-B) Representative images from four biologically independent experiments. (C) Extent of enrichment or depletion of EGFP-tagged proteins at single VLP assembly sites. Multiple VLPs (*n*=12 for each protein) were analyzed and data are shown as mean ± SD. (D) Cells stably expressing MLVenv-ΔPalm-EGFP were transfected with Gag and Gag-mCh and imaged by TIRF-M. (Left) Time series of MLVenv-ΔPalm distribution at VLP assembly site during biogenesis of

single VLP. (Right) Time trace of normalized fluorescence intensities of assembling VLP (magenta) and MLVenv-ΔPalm (green) at the single VLP assembly site shown at right. (E) Cells transfected with Gag and Gag-mCh were labeled with NBD-SM and imaged by TIRF-M. Time-series panels showing redistribution of NBD-SM at single VLP assembly sites during biogenesis of VLPs. (F) Cells stably expressing EGFP-GG were transfected with Gag and Gag-mCh and imaged by TIRF-M. (Left) Time series showing the redistribution of EGFP-GG at assembly site during biogenesis of single VLP. (Right) Time trace of normalized fluorescence intensity of assembling VLP (labeled with Gag-mCh, magenta) and EGFP-GG (green) at single VLP assembly site. (D-F) Representative images from two biologically independent experiments. (G) Normalized time of redistribution (τ_r) of indicated proteins at single VLP assembly sites. Data are shown as mean ± SEM for *n* individual single VLPs drawn from two biologically independent experiments. *n*=39, GG; *n*=24, MS2; *n*=38, CHMP4B. Scale bar, 10 μm (A), 1 μm (E).

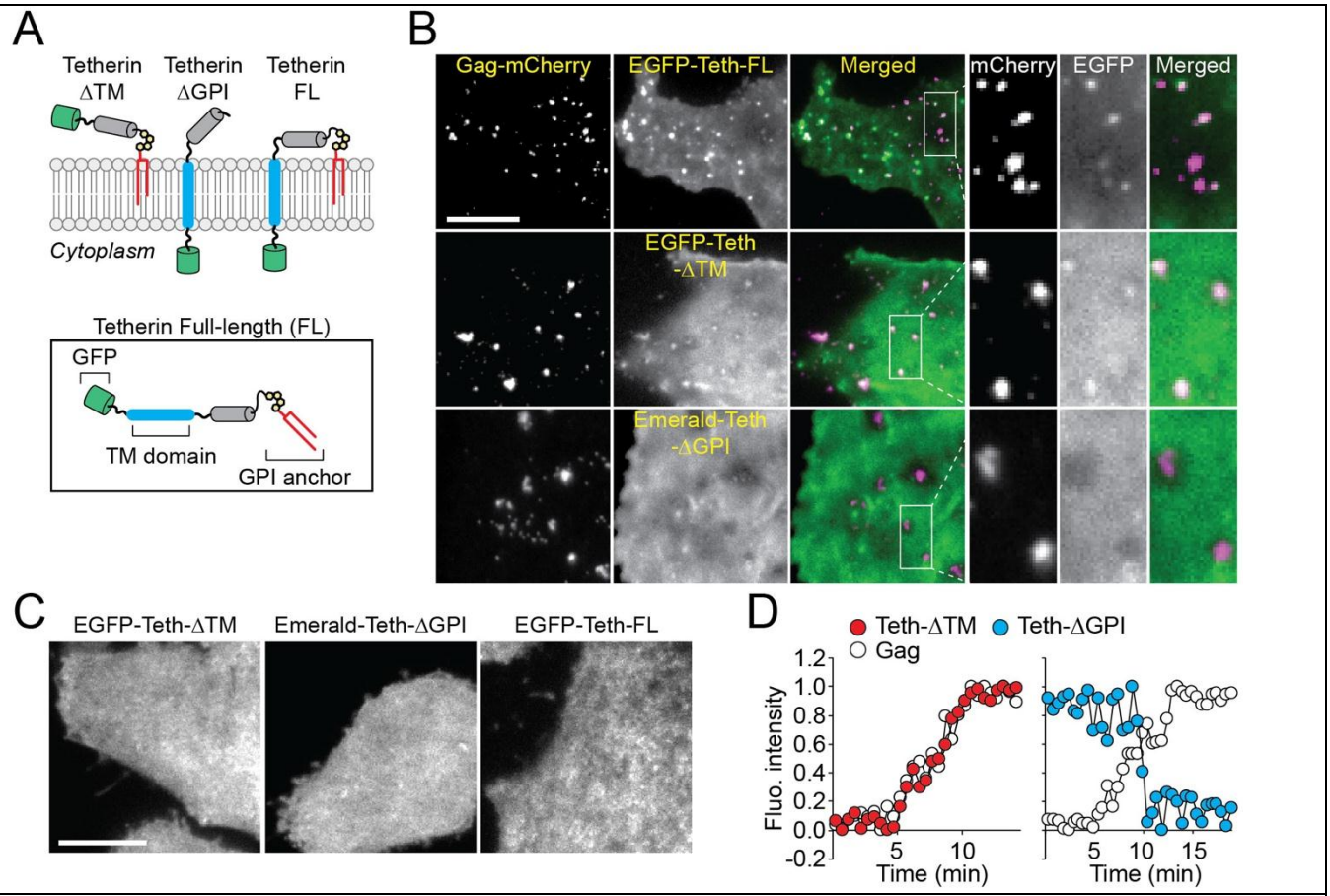

Supplementary Figure 4

Redistribution of tetherin constructs between bulk PM and VLP assembly sites.

(A) Schematic illustrating membrane anchors and topology of full-length and mutant tetherin constructs used in the study. (B) TIRF-M images showing the distribution of EGFP-fusions of indicated tetherin constructs during assembly of VLPs at PM of COS-7 cells. Gag-mCh labels sites of VLP assembly. (C) TIRF-M images of steady state distribution of indicated tetherin constructs on the PM of HeLa cells. (D) Normalized fluorescence intensity traces of Gag-mCh (open circles), tetherin-ΔTM (red), or, tetherin-ΔGPI (blue) at VLP assembly site during assembly of single VLP. (B-D) Representative images from two biologically independent experiments. Scale bar, 10 μm.

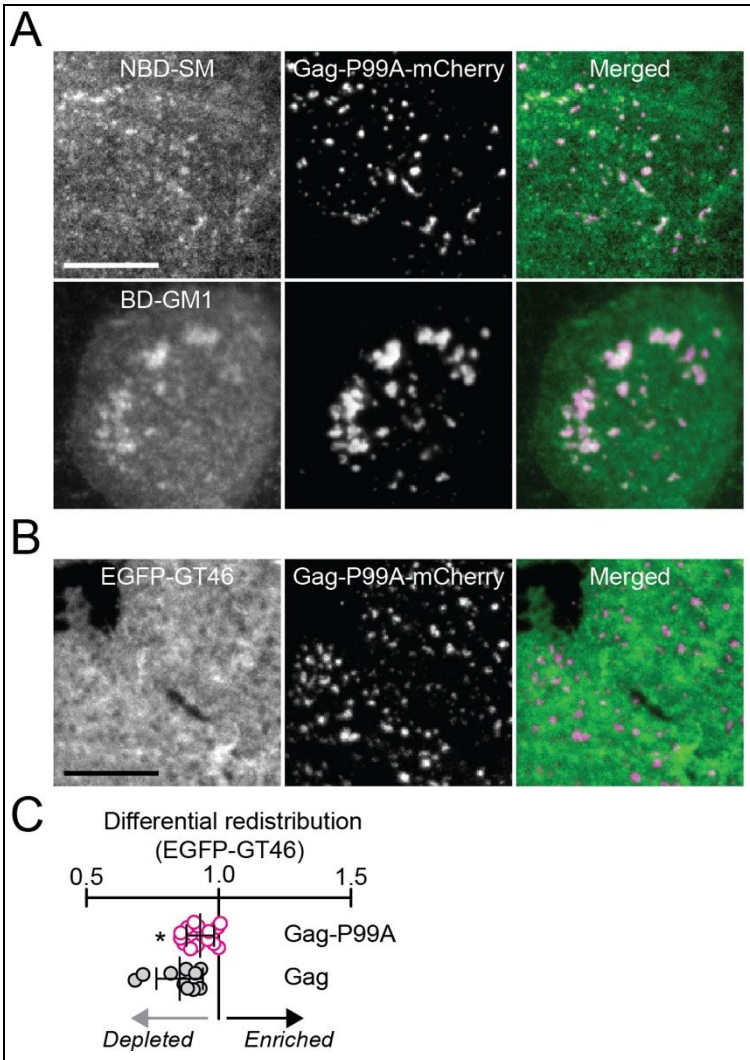

Supplementary Figure 5

Increased curvature of assembly site membrane mediates late stage redistribution of proteins.

(A) TIRF-M images of NBD-SM (top panel) and BD-GM1 (bottom panel) distribution on PM of cells during formation of Gag-P99A assembly platforms. Gag-P99A assembly sites are labeled by Gag-P99A-mCh. (B) TIRF-M image showing distribution of EGFP-GT46 on PM of cells during formation of Gag-P99A assembly sites marked by Gag-P99A-mCh. (A, B) Representative images from two biologically independent experiments. (C) Extent of depletion of EGP-GT46 at wild type Gag assembly sites and Gag-P99A platforms compared to bulk PM. Multiple cells were analyzed and data are shown as mean ± SD for *n* individual cells; two-sided Student's *t*-test, p=0.01. Gag-P99A: n=15; Gag: n=10. Scale bar, 10 µm.

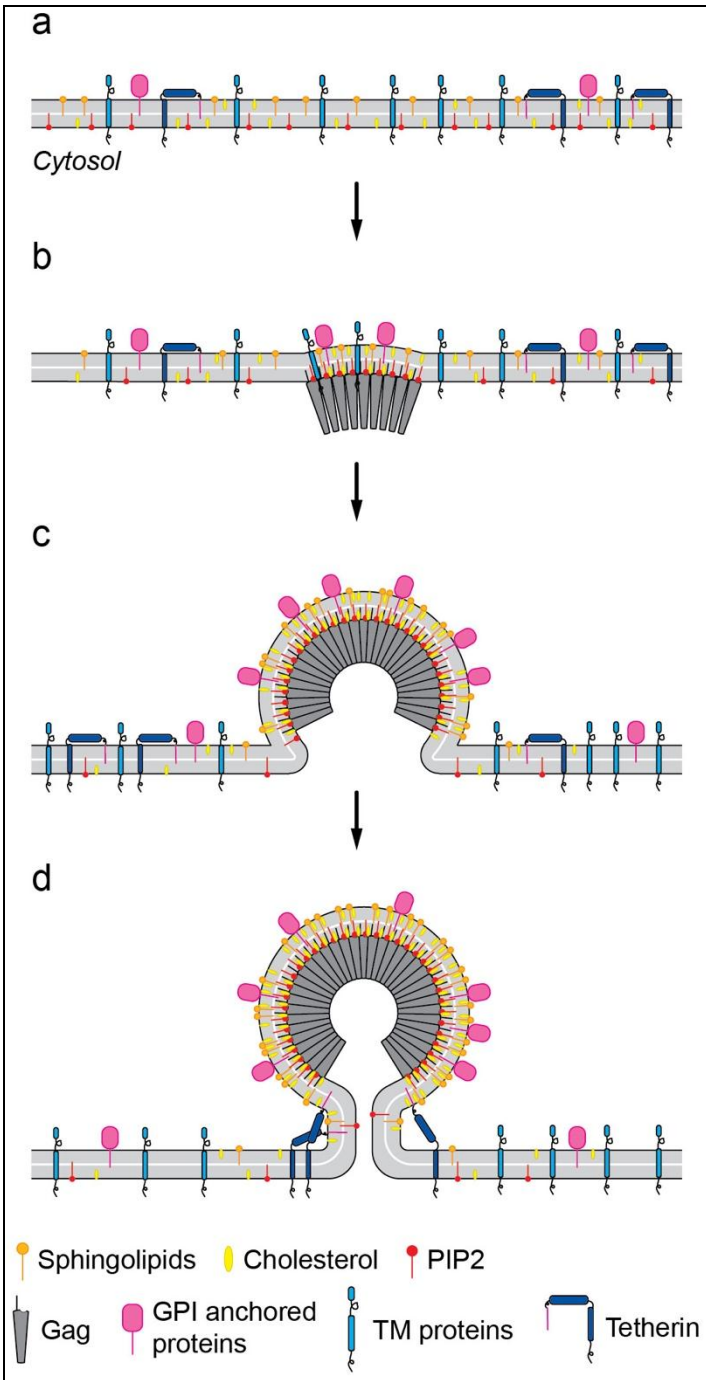

Supplementary Figure 6

Proposed model for sorting of host cell PM proteins into HIV membrane.

The panels illustrate the evolution of the viral assembly site membrane. (a) PM proteins are homogenously distributed and diffraction-limited TIRF-M does not detect any preexisting microdomains enriched in specific proteins. (b) Following membrane binding and oligomerization of

Gag at viral assembly site, PIP2 molecules in inner leaflet of PM are clustered at the assembly site via their interaction with highly basic region of Gag molecules. PIP2 at assembly site recruits outer leaflet lipids and GPI-APs with long, saturated lipid chains to the assembly site by transbilayer coupling, which in turn generates ordered lipid domain with Lo-phase like characteristics at the assembly site. Ordered lipid preferring PM proteins begin to preferentially partition into this ordered assembly site. (c) Redistribution of proteins and the increasing curvature of assembly site membrane helps to enhance the phase separation of the viral assembly site and leads to further sorting of proteins including depletion of disordered lipid-phase (L_d-phase) preferring proteins from the assembly site. (d) Proteins with dual membrane anchors such as tetherin are recruited to the viral assembly site at the end of the assembly process after the assembly site membrane has acquired high membrane curvature.

Captions for Supplementary Videos

Supplementary Video 1. Single VLP assembly. TIRF-M time series of a cell expressing a combination of HIV Gag-mCh and unlabeled Gag (at 1:10 ratio) illustrating the assembly of single VLP particles on the plasma membrane. The cell was imaged 8h post transfection with Gag plasmids. Representative video from three biologically independent experiments.

Supplementary Video 2. Recruitment of EGFP-CD59 to single VLP assembly site. Movie of single VLP assembly illustrating the recruitment of EGFP-CD59 (right, green channel) to VLP assembly site (marked by Gag-mCh, left, red channel). Representative video of 52 VLPs drawn from two biologically independent experiments.

Supplementary Video 3. Recruitment of MLV-Env to single VLP assembly site. Movie of single VLP assembly illustrating the recruitment of MLVenv-EGFP (right, green channel) to VLP assembly site (marked by Gag-mCh, left, red channel). Representative video of 62 VLPs drawn from two biologically independent experiments.

Supplementary Video 4. Depletion of EGFP-GT46 from single VLP assembly site. Movie of single VLP assembly illustrating the depletion of EGFP-GT46 (right, green channel) from VLP assembly site containing Gag-mCh (left, red channel). Representative video of 54 VLPs drawn from two biologically independent experiments.

Supplementary Video 5. Recruitment of tetherin single VLP assembly site. Movie of single VLP assembly illustrating the recruitment of EGFP-tetherin (right, green channel) to VLP assembly site (marked by Gag-mCh, left, red channel). Representative video of 46 VLPs drawn from two biologically independent experiments.

Supplementary Table Legends

Supplementary Table 1. Statistics Source Data. Source data for Fig. 1-6 and Supplementary Fig. 1-5.